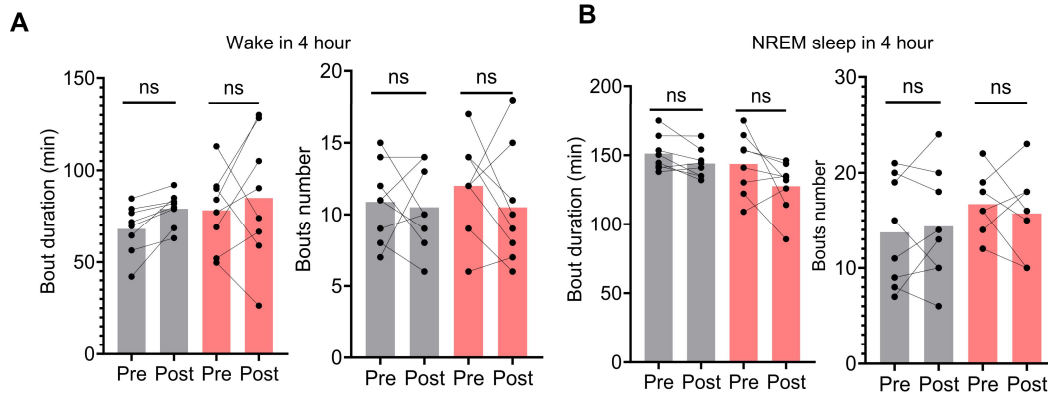


1 **Oxytocin modulates inhibitory balance in the prelimbic cortex to**
2 **support social memory consolidation during REM sleep**

3 †Yanchao Liu et al. Email: yanchao_liu@whu.edu.cn

4 ‡Corresponding author. Email: zqp005098@whu.edu.cn (Q.-P.Z.);
5 gaoyangbest@whu.edu.cn (Y.G.); xuhaibo@whu.edu.cn (H.-B.X.)

6



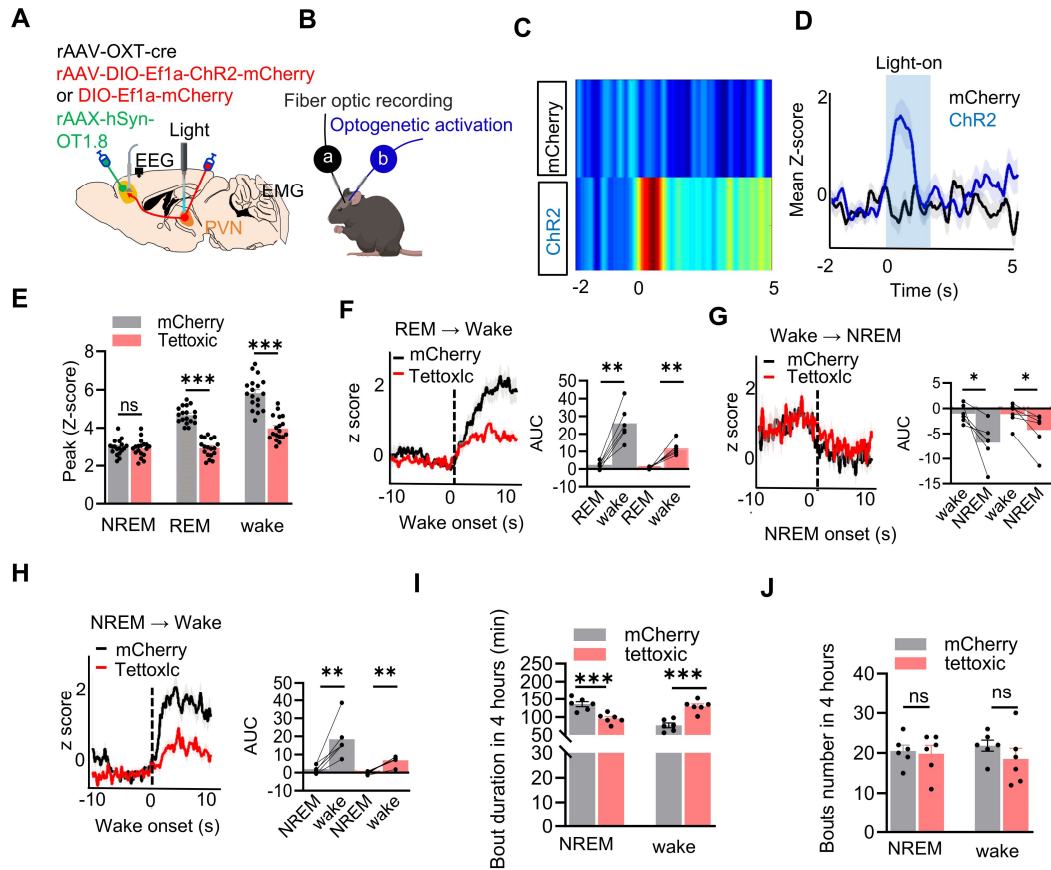
8

8 **Figure S1. OXT receptor antagonists did not affect NREM sleep and wake.**

9 (A and B) Bilateral antagonism of OXT receptors in PrL did not affect wake (A) and
10 NREM sleep (B) in mice. $n = 8$, $ns, p > 0.05$, as determined by unpaired t-test. Data are
11 expressed as mean \pm SEM.

12

13



14

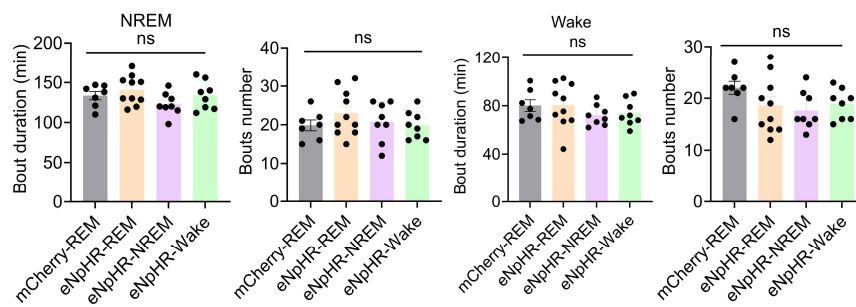
15 **Figure S2. Population activity of PVN^{OXT} neurons affected OXT release in PrL,**
 16 **wake and NREM sleep.**

17 (A to D) Schematic of optogenetics virus injection, photostimulation and fluorescence
 18 recordings. Peri-event plots illustrate the averaged fluorescence z scores of mcherry
 19 group (n = 4) and ChR2 group (n = 4) in response to photostimulation of PVN^{OXT}
 20 neurons (473 nm laser, a train of ten 10-ms light pulses at 10 HZ, 1s on and 50 s off for
 21 20 min, blue vertical bars). The curves and shaded regions indicate the mean ± SEM.

22 (E) Comparison of peak OXT biosensor fluorescence signal during wake, NREM sleep,
 23 and REM sleep in mCherry and tettoxic group. n=18, three sessions per mouse from 6
 24 mice; ns, $p > 0.05$; *** $p < 0.001$, as determined by unpaired t-test.

25 (F to H) OXT biosensor fluorescence signal transformation aligned to sleep-wake state
 26 transitions. Comparison of AUC over 10 s during wake, NREM, and REM sleep. * $p <$
 27 0.05 ; ** $p < 0.01$, as determined by paired t-test.

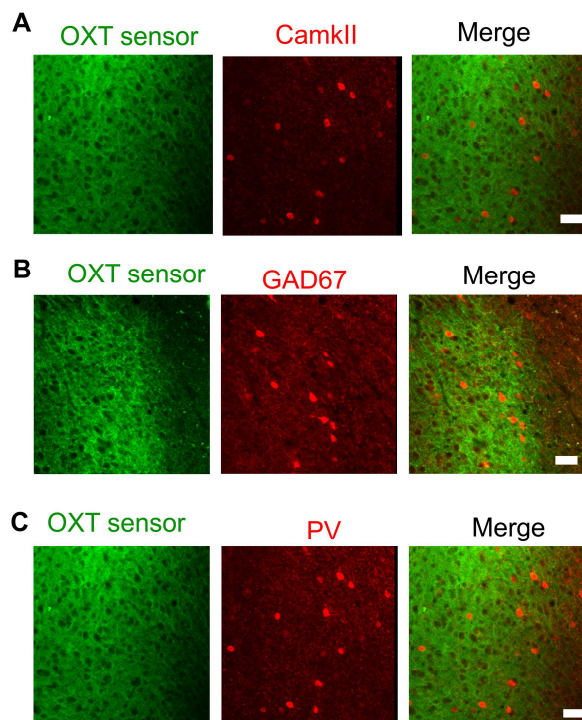
28 (I and J) Duration and bouts of NREM Sleep and wake over a 4-hour in two groups of
 29 mice. ns, $p > 0.05$; *** $p < 0.001$, as determined by unpaired t-test.



31

32 **Figure S3. Photoinhibition of PVN^{OXT}-PrL pathway during REM sleep/NREM**
 33 **sleep/wake phase did not affect NREM sleep and wake.**

34 mCherry-REM group, n = 7 mice; eNpHR-REM group, n = 10 mice; eNpHR-NREM
 35 and eNpHR-Wake groups, n = 8 mice each; ns, $p > 0.05$, as determined by unpaired t-
 36 test. Data are expressed as mean \pm SEM.



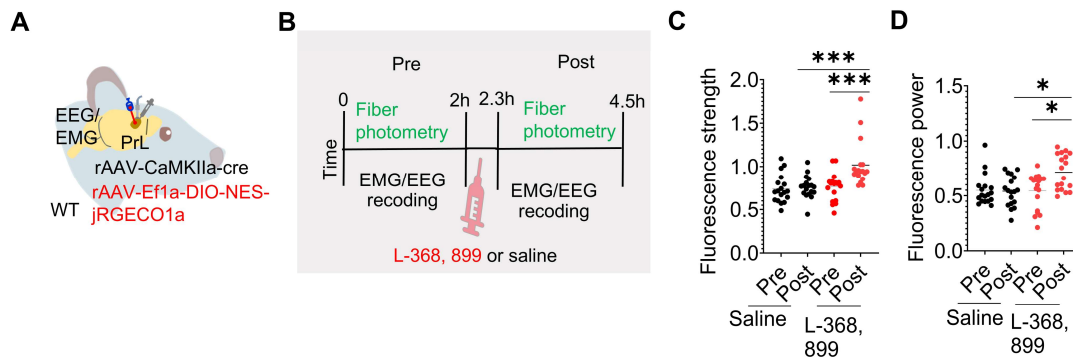
37

38 **Figure S4. OXT receptor distribution on excitatory and inhibitory neurons.**

39 **A.** Representative photomicrograph OXT sensor in PrL (left, green), CamkII
 40 immunolabeling (middle, red) and merged image (right). n = 2 mice. Scale bar = 200
 41 μ m.

42 **B.** Fluorescence images of OXT sensor in PrL (left, green), immunostaining of GAD67
 43 (middle, red) and merged image (right). n = 2 mice. Scale bar = 200 μ m.

44 C. Representative image of OXT sensor in PrL (left, green), PV immunolabeling
 45 (middle, red) and merged image (right). n = 2 mice. Scale bar = 200 μ m.

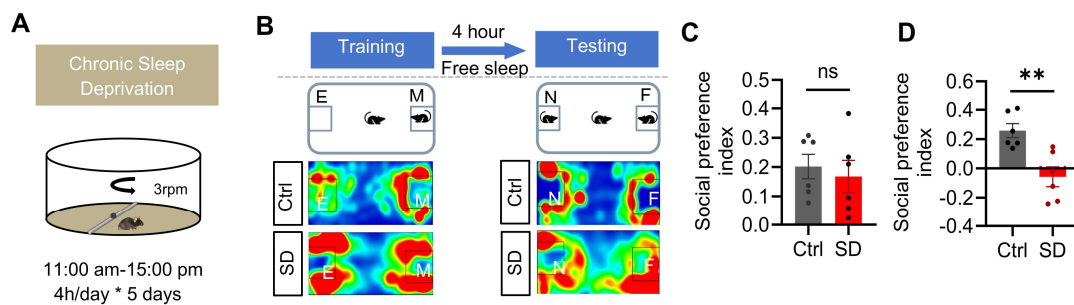


46
 47 **Figure S5. Higher Ca^{2+} activity in pyramidal neurons was observed during REM**
 48 **sleep after local OXT receptor antagonism treatment in PrL.**

49 (A) Diagram illustrating virus injection, cannula placement, setup for fiber photometry
 50 and EMG/EEG recording in mice.

51 (B) Timeline showing administration of L-368, 899 (OXT receptor antagonist) or saline.

52 (C and D) Comparison of fluorescence strength (C), fluorescence power (D) of PYR
 53 neurons Ca^{2+} signal before and after application of L-368, 899 or saline during REM
 54 sleep. n=18, three sessions per mouse from 6 mice; * $p < 0.05$; *** $p < 0.001$, as
 55 determined by paired and unpaired t-test.

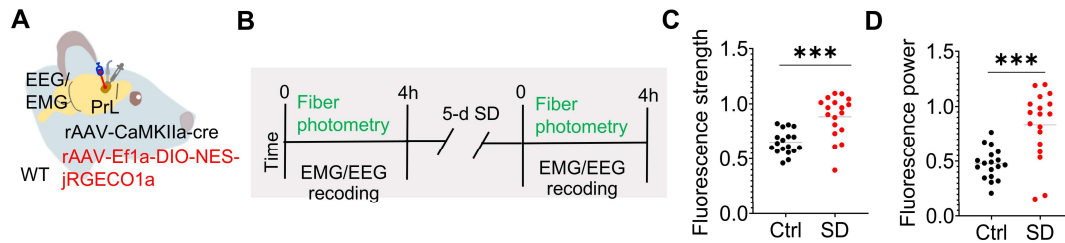


56
 57 **Figure S6. Chronic SD impaired social memory in mice.**

58 (A) Protocol for chronic SD.

59 (B) Upper, two-choice social memory test. E, empty; M, mice; N, novel mice; F,
 60 familiar mice. Lower, representative heatmaps of distribution of time in two-choice task.

61 (C and D) Social preference index was assessed by two-choice social novelty test in
 62 training (C) and testing (D) phase, respectively. n = 6 mice; ns, $p > 0.05$; ** $p < 0.01$,
 63 as determined by unpaired t-test.



64

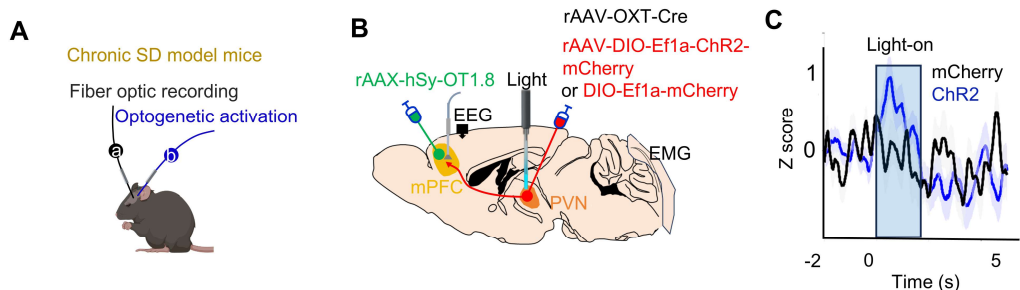
65 **Figure S7. Higher Ca^{2+} activity in pyramidal neurons in PrL was observed during**
 66 **REM sleep in chronic SD mice.**

67 (A) Diagram illustrating virus injection, setup for fiber photometry and EMG-EEG
 68 recording in mice.

69 (B) Schematic of Fiber photometry and EMG-EEG recording.

70 (C and D) Comparison of fluorescence strength (C), fluorescence power (D) of PYR
 71 neurons Ca^{2+} signal during REM sleep between Ctrl and SD group. $n = 18$, three
 72 sessions per mouse from 6 mice; $***p < 0.001$, as determined by unpaired t-test.

73

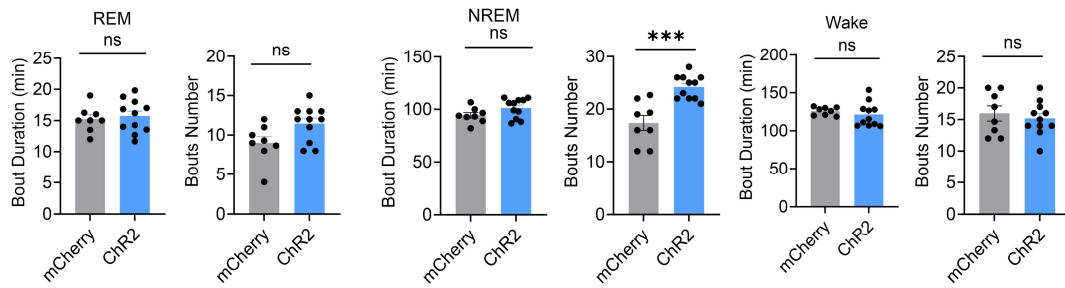


74

75 **Figure S8. OXT fluorescence in PrL increased after the activation of PVN^{OXT}**
 76 **neurons in SD mice.**

77 (A and B) Schematic of optogenetics virus injection, photostimulation and fluorescence
 78 recordings in SD mice.

79 (C) OXT fluorescence in PrL increased after the activation of PVN^{OXT} neurons in SD
 80 compared with mCherry ($n = 4$, 473 nm laser, a train of ten 10-ms light pulses at 10 Hz,
 81 1 s-on and 50 s-off for 20 min, blue vertical bars). The curves and shaded regions
 82 indicate the mean \pm SEM.

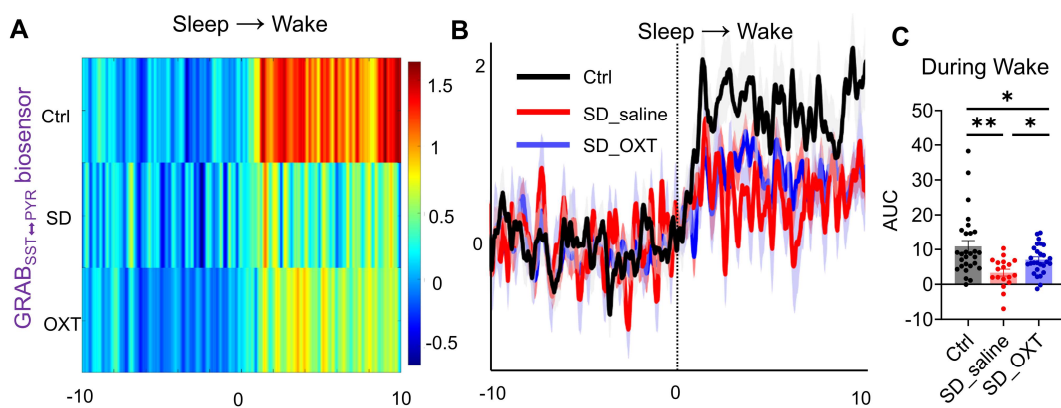


83

84 **Figure S9. Optogenetic activation of PVN^{OXT}-PrL pathway during REM sleep did**
 85 **not affect sleep and wake duration in SD mice.**

86 Photoactivation of the PVN^{OXT}-PrL pathway during REM sleep could affect sleep-wake
 87 with a slightly higher number of REM and NREM occurrences. n = 8 mice in mCherry
 88 group; n = 11 mice in Chr2 group; ns, $p > 0.05$; * $p < 0.05$; ** $p < 0.01$, as determined
 89 by unpaired t-test.

90



91

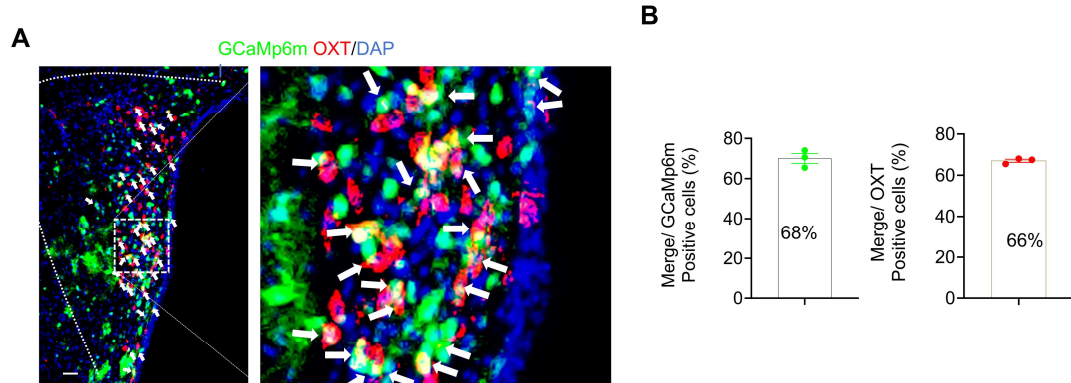
92 **Figure S10. Intranasal OXT restored reduced SST release in PrL in SD mice.**

93 **(A)** Individual transitions with color-coded fluorescence intensity from sleep to wake
 94 in three groups.

95 **(B)** Mean \pm SEM activity profiles of GRAB_{SST \leftrightarrow PYR} biosensor in PrL during the
 96 transition from sleep to wake. (black = ctrl, red = SD_saline, blue = SD_OXT).

97 **(C)** AUC comparisons of GRAB_{SST2.0 \leftrightarrow PYR} biosensor activity in PrL during wake. Ctrl,
 98 n = 28 trials from 5 mice; SD_saline, n = 18 trials from 4 mice; SD_OXT, n = 27 trials
 99 from 4 mice; * $p < 0.05$, ** $p < 0.01$, as determined by One-way ANOVA.

100



101

102 **Figure S11. The specificity and efficiency of the OXT-promoter-driven virus**
 103 **construct.**

104 (A) Overlap between GCaMP6m and immunostaining of OXT in the PVN.

105 Representative photomicrographs of PVN^{OXT} neurons from a mouse microinjected with
 106 rAAV-OXT-Cre and AAV-DIO-hSyn-GCaMP6m at the PVN. The GCaMP6m (green)
 107 and OXT immunolabeling (red) indicate GCaMP6m and OXT-expressing neurons,
 108 respectively, and the yellow image depicts merged neurons. Scale bar = 200 μ m.

109 (B) Percentage of Gcamp6m (green)/OXT double-positive cells versus Gcamp6m
 110 positive cells (left) or versus OXT-positive cells (right). n = 3 mice.

111

KEY RESOURCES TABLE

REAGENT RESOURCE	or	SOURCE	IDENTIFIER
Antibodies			
Alexa Fluor 546 donkey anti-rabbit		Servicebio	GB21303
Alexa Fluor 546 donkey anti-mouse		Servicebio	GB21301
mouse anti-CamKII		Cell signaling	3362
mouse anti-GAD67		Sigma	MAB5406
mouse anti-Parvalbumin		Sigma	SAB4200545
rabbit anti-Oxytocin- neurophysin 1		abcam	EPR20973

Virus		
rAAV9-hSyn-OT1.8	Brain case Co., Ltd.	Cat#BC-1119
rAAV2/9-camkII-SST2.0	BrainVTACo.,Ltd.	Cat#PT-7175
rAAV2/9-DIO-VIP1.7	BrainVTACo.,Ltd.	Cat#PT-8304
rAAV-CaMKIIa-CRE-WPRE-hGH polyA	BrainVTACo.,Ltd.	Cat#PT-0220
Raav-EF1a-DIO-NES-jRGECO1a	Brain case Co., Ltd.	Cat#BC-0212
rAAV2/9-OXT-Cre-WPRE-hGH-pA	BrainVTACo.,Ltd.	Cat#PT-6086
rAAV2/9-CAG-DIO-axon-jGCaMP7b	BrainVTACo.,Ltd.	Cat#PT-8161
rAAV-EF1a-DIO-synaptophysin-jGCaMP7b	Brain case Co., Ltd.	Cat#BC-1378
rAAV2/9-DIO-EF1a-hChR2 (H134R)-mCherry	BrainVTACo.,Ltd.	Cat#PT-3787
rAAV2/9-DIO-EF1a-eNpHR3.0-mCherry	BrainVTACo.,Ltd.	Cat#PT-0007
rAAV2/5- EF1a-DIO-tetotoxicP2A-mcherry	BrainVTACo.,Ltd.	Cat#PT-2139
rAAV-EF1a-DIO-GCaMp6m-WPRE-hGH polyA	BrainVTACo.,Ltd.	Cat#PT-0283
rAAV2/9-DIO-Ef1a-mCherry	BrainVTACo.,Ltd.	Cat#PT-0115
Animals		
Mouse: C57BL/6J	Beijing Vital River	SCXK: 2022-0030

		Laboratory Animal Technology Co., Ltd.	
Mouse: (C57BL/6)	PV-Cre	Beijing Vital River Laboratory Animal Technology Co., Ltd.	Gifted by Professor Jianzhi Wang's research group
Mouse: (C57BL/7)	VIP-Cre	Genepax Biotechnology Co., Ltd	GAP1043